

Spectral Properties of δ -Plutonium: Sensitivity to $5f$ Occupancy

Jian-Xin Zhu,¹ A. K. McMahan,² M. D. Jones,³ T. Durakiewicz,¹ J. J. Joyce,¹ J. M. Wills,¹ and R. C. Albers¹

¹*Los Alamos National Laboratory, Los Alamos, New Mexico 87545, USA*

²*Lawrence Livermore National Laboratory, Livermore, California 94550, USA*

³*University at Buffalo, SUNY, Buffalo, New York 14260, USA*

(Dated: February 1, 2008)

By combining the local density approximation (LDA) with dynamical mean field theory (DMFT), we report a systematic analysis of the spectral properties of δ -plutonium with varying $5f$ occupancy. The LDA Hamiltonian is extracted from a tight-binding (TB) fit to full-potential linearized augmented plane-wave (FP-LAPW) calculations. The DMFT equations are solved by the exact quantum Monte Carlo (QMC) method and by the Hubbard-I approximation. We demonstrate strong sensitivity of the spectral properties to the $5f$ occupancy, which suggests using this occupancy as a fitting parameter in addition to the Hubbard U . By comparing with photoemission data, we conclude that the “open shell” $5f^5$ configuration gives the best agreement, resolving the controversy over $5f$ “open shell” versus “close shell” atomic configurations in δ -Pu.

PACS numbers: 71.20.Gj, 71.27.+a, 75.20.Hr, 79.60.-i

I. INTRODUCTION

From a consideration of its condensed matter physics properties, crystal structure, and metallurgy, plutonium is probably the most complicated element in the periodic table,^{1,2,3,4,5,6} including a phase diagram with six allotropic phases. The low-temperature monoclinic α -phase is stable up to 395 K while the face-center-cubic (fcc) δ -phase is stable between 592 and 724 K. Furthermore, in stabilized alloys the α to δ phase transformation of Pu has a significant volume expansion, with the δ -phase 25% larger in volume than the α -phase. This behavior is related to the special position of Pu in the periodic table, which is at the boundary between the light actinides that have itinerant $5f$ electrons and the heavy actinides with localized $5f$ electrons. In this situation the electrons are in a very strongly correlated state where even the best conventional LDA band-structure calculations cannot predict its unique properties, e.g., the δ -phase volume^{7,8} in the experimentally observed non-magnetic state. This failure has stimulated numerous attempts to include additional electronic correlation effects. Although LDA theory has repeatedly claimed^{9,10,11,12,13} that the thermal expansion in Pu is a consequence of magnetism, this is in striking contradiction with experimental data.¹⁴ Several research groups^{15,16,17} have applied the LDA+ U method to include more f - f correlation energy. By adjusting the on-site Coulomb repulsion energy (U) appropriately, it has been possible to fit to the experimental δ -phase volume. The LDA+ U calculations also indicated an instability of δ -Pu toward an antiferromagnetic ground state. More recent calculations based on the “around-mean-field” LSDA+ U including the spin-orbit interaction¹⁸ or the fully-localized-limit LSDA+ U quenched the spin polarization through an $\approx f^6$ configuration, and obtained the correct δ -phase volume due to a weak exchange interaction.¹⁹ To predict the correct volume, a mixed-level model has also been proposed by one of us together with co-workers.²⁰ In this model, four of

the five $5f$ electrons in the δ -phase were constrained to be localized and were not allowed to hop from site to site, but could hybridize with the conduction electrons. A major advance came when a new calculation scheme was proposed to merge LDA-based methods with DMFT.^{21,22} DMFT^{23,24} is a many-body technique that is able to treat the band- and atomic-like aspect simultaneously when applied to plutonium. Within the LDA+DMFT approach,^{22,25} the origin of substantial volume expansion was explained in terms of the competition between Coulomb repulsion and kinetic energy. Thus, two dramatically different pictures for the non-magnetism of δ -Pu have emerged. In the “ $5f^6$ ” picture,^{18,19,26,27} by including the spin-orbit interaction, one starts with a closed $f^{5/2}$ atomic subshell fully filled with six electrons while the $f^{7/2}$ subshell is empty, making Pu magnetically inert. In the “ $5f^5$ ” picture,^{25,28} one starts with an open $f^{5/2}$ atomic subshell filled with five electrons, resulting in a magnetic moment that should be screened by the sd valence electrons. Therefore, more studies are necessary to determine which picture will prevail.

In this paper, we report a systematic LDA+DMFT study of the spectral properties of δ -Pu with varying $5f$ occupancy. Throughout this work, the LDA part of Hamiltonian is determined from a new TB fit to FP-LAPW calculations. The DMFT equations are solved using quantum Monte Carlo (QMC) simulations as well as the more approximate Hubbard-I method. These provide an accurate characterization of spectral properties of δ -Pu. It is found that the $5f$ spectral density of Pu is very sensitive to its occupancy. Good agreement is found with photoemission spectroscopy (PES) measurements when about five electrons occupy the $f^{5/2}$ subshell, in support of the second picture. Other recent work appears also to be in support of this picture. Measurements of the branching ratio in $5d$ to $5f$ transitions favor a $5f$ count closer to 5 than 6,^{29,30} while subsequent LDA+DMFT calculations²⁸ using a vertex-corrected one-crossing approximation for the auxiliary impurity problem yield re-

sults for the branching ratio in agreement with experiment²⁹ and suggest a 5f occupancy of 5.2. Similarly, specific heat calculations carried out using an LDA+DMFT method with a perturbative T -matrix and fluctuating exchange approach to the auxiliary impurity problem also favor the $\sim 5f^5$ configuration.³¹

The remainder of this paper is organized as follows: Theoretical methods are given in Sec. II; numerical results for the δ -Pu are presented in Sec. III; and then a summary follows in Sec. IV

II. THEORETICAL METHODS

Most LDA+DMFT methods to date have been implemented in a basis of linear muffin-tin orbitals (LMTO) within the atomic sphere approximation (ASA), or in its full potential version. Here we use an alternative version of the LDA+DMFT method, which is based on a recently developed TB theory.³² In this representation, the full second-quantized Hamiltonian is written as:

$$\hat{H} = \sum_{\mathbf{k}, ljm_j, l'j'm'_j} [H^0(\mathbf{k})]_{ljm_j, l'j'm'_j} \hat{c}_{\mathbf{k}ljm_j}^\dagger \hat{c}_{\mathbf{k}l'j'm'_j} + \frac{U_f}{2} \sum_{i, j, m_j \neq j', m'_j} \hat{n}_{ifjm_j} \hat{n}_{ifj'm'_j}. \quad (1)$$

Here \mathbf{k} are the Brillouin-zone wavevectors; i are lattice site indices; l is the orbital angular momentum; j is the total angular momentum; $m_j = -j, -j+1, \dots, j-1, j$; $\hat{n}_{ifjm_j} \equiv \hat{c}_{ifjm_j}^\dagger \hat{c}_{ifjm_j}$. The relevant orbitals for Pu are 7s, 6p, 6d, and 5f, and so the matrices $\hat{H}^0(\mathbf{k})$ are 32×32 . They are given by

$$\hat{H}^0(\mathbf{k}) = \hat{H}^{\text{LDA}}(\mathbf{k}) + (\varepsilon_f - \varepsilon_f^{\text{LDA}}) \hat{I}_f. \quad (2)$$

Here the matrix \hat{I}_f is zero except for 1's along the 14 f-f diagonals, and

$$\varepsilon_f^{\text{LDA}} = \frac{1}{14N} \sum_{\mathbf{k}} \text{Tr}[\hat{H}^{\text{LDA}}(\mathbf{k}) \hat{I}_f], \quad (3)$$

where N is the number of \mathbf{k} points in the Brillouin zone. The matrices $\hat{H}^{\text{LDA}}(\mathbf{k})$ are orthogonalized, single-electron Hamiltonian matrices obtained from TB fits to the FP-LAPW calculations.³² In this study, strict orthogonality is maintained between the TB orbitals (hence no overlap matrix need be included). All matrices are calculated at the experimental δ -Pu volume.

The Slater-Koster tables for the sp^3d^5 matrix elements can be found in standard references,^{33,34} and we have used an extended formalism for a unified treatment including additional matrix elements involving f-electrons.³⁵ Typical TB calculations are then reduced to using TB as an interpolation scheme; the matrix elements are determined by fitting to *ab-initio* calculated quantities such as the total energy and band energies. In this

study TB inter-site parameter values are evaluated at inter-atomic distances out to the fifth nearest neighbor, resulting in 100 inter-site parameters and 4 on-site parameters. The effect of the spin-orbit interaction is included as a perturbation, with its parameters kept fixed across the bands, although evaluated at the most important energies, namely at the respective centers of gravity of the occupied state density for each orbital type.³⁶ The spin-orbit coupling adds 3 more parameters to the TB fit, resulting in a total of 107 parameters (parameter values are available on request from the authors). The quality of the present TB fit for δ -Pu is comparable to that shown elsewhere for fcc U.³²

As customary in LDA+DMFT calculations, Eqs. (1-3) presume that the LDA results are sufficient for both the off-diagonal elements of $\hat{H}^0(\mathbf{k})$ (hybridization) and the diagonal elements of the assumed uncorrelated *spd* electrons. For the correlated f electrons one needs of course the Coulomb interaction as seen in Eq. (1), but in addition, since the LDA site energy defined by Eq. (3) includes Coulomb contributions, it must be replaced by the true or bare site energy ε_f as in Eq. (2). Both ε_f and U_f may be estimated from the dependence of the LDA site energy $\varepsilon_f^{\text{LDA}}(n_f)$ on f occupation n_f via LDA constrained occupation calculations,^{37,38} and comparison to spectroscopic data for ions suggests uncertainties of ± 1 eV in such results for both quantities.³⁷ Typical values of U_f are around 4 eV for δ -Pu, as we also find, and this value is assumed throughout the present paper. Given the sensitivity of n_f to ε_f , on the other hand, we have chosen to adjust the parameter ε_f in the present work as a natural and convenient means of exploring the sensitivity of the δ -Pu spectra to 5f occupancy.³⁹ This adjustment amounts to varying the double counting term in conventional LDA+ U or LDA+DMFT terminology.

Within the DMFT, the lattice problem Eq. (1) is mapped onto a multi-orbital quantum single impurity problem subject to a self-consistency condition:

$$\hat{\mathcal{G}}^{-1}(i\omega_n) = \hat{G}_{\text{loc}}^{-1}(i\omega_n) + \hat{\Sigma}(i\omega_n). \quad (4)$$

Here $\hat{\mathcal{G}}(i\omega_n)$ is the Weiss function, $\hat{\Sigma}(i\omega_n)$ is a \mathbf{k} -independent self-energy, and the local Green's function is defined as $\hat{G}_{\text{loc}}(i\omega_n) = \sum_{\mathbf{k}} \hat{G}_{\mathbf{k}}(i\omega_n)/N$, where the lattice Green's function reads

$$\hat{G}_{\mathbf{k}}(i\omega_n) = [(i\omega_n + \mu) \hat{I} - \hat{H}^0(\mathbf{k}) - \hat{\Sigma}(i\omega_n)]^{-1}, \quad (5)$$

with \hat{I} the 32×32 unit matrix and μ the chemical potential. Since we have restricted strong correlation to the f orbitals only, it is customary to take $\hat{\Sigma}$ to have nonzero elements only within the 14×14 f-f block, which permits a similar reduction in the quantum single-impurity problem itself. Furthermore, we neglect the off-diagonal elements in the self-energy and, by ignoring the crystal-field effect in the impurity problem, treat the $5f_{j=5/2}$ levels as one 6-fold degenerate level and the $5f_{j=7/2}$ as another 8-fold degenerate level. The only nonzero f-f

block self-energy reduces to

$$\Sigma_{jm_j, j'm'_j}^{ff}(i\omega_n) = \Sigma_j^{ff}(i\omega_n) \delta_{jj'} \delta_{m_j m'_j}, \quad (6)$$

and we need only find functions for the two spin-orbit states $j = 5/2$ and $j = 7/2$. Note that when no spin-orbit coupling is included, $\Sigma_{5/2}^{ff}(i\omega_n) = \Sigma_{7/2}^{ff}(i\omega_n)$. Correspondingly, the local Green's functions is dictated by:

$$G_{\text{loc}, jm_j, j'm'_j}^{ff}(i\omega_n) = \frac{\delta_{jj'} \delta_{m_j m'_j}}{(2j+1)N} \sum_{\mathbf{k}} \text{Tr}_{fj} \{ \hat{G}_{\mathbf{k}}(i\omega_n) \}. \quad (7)$$

It should also be noted that we neglect the crystal-field effects only at the auxiliary impurity problem, all such effects are still retained in $\hat{H}^0(\mathbf{k})$, where hybridization dominates anyway.

To solve the auxiliary impurity problem, we have employed both the Hubbard-I approximation and an implementation of the QMC method that has been used to study properties of the compressed lanthanides.^{40,41,42} The former method is more approximate but much faster while the latter is more rigorous but computationally more expensive. The Hubbard-I approximation is also useful in various ways: it is more applicable in the large-volume atomic limit, where it gives insight into the atomic aspects of Pu; it provides a good initial guess for the DMFT(QMC) simulations; and it makes it possible to examine the full f - f Coulomb interaction (all four Slater integrals F^k) and its consequent term structure in DMFT(HI) in contrast to DMFT(QMC), where it is still difficult to go beyond just the standard Hubbard $U_f \equiv F^0$. Unless specifically noted otherwise, all DMFT(HI) and DMFT(QMC) results reported in this paper include only U_f in addition to the spin-orbit interaction. For the DMFT(QMC) calculations, we used 6000 sweeps per QMC iteration for the imaginary time segments $L = 112$ at a temperature $T = 632$ K, which is about as low a temperature as is practical at the present time with QMC, and performed at least 100 iterations. To improve the input data needed for the maximum entropy (MaxEnt) analytical continuation,⁴³ at the last iteration, we dramatically increased the number of sweeps such that the number of bins, each containing 100 measurements, is larger than $2L$.

III. RESULTS

In Fig. 1 we show the spectral density of δ -Pu at $T = 632$ K for various values of the $5f$ occupancy n_f . The left three panels display underlying atomic properties obtained from the DMFT(HI) calculations, consistent with a ground state $\alpha|f_{5/2}^5\rangle + \beta|f_{5/2}^6\rangle$, where $|\alpha|^2 + |\beta|^2 = 1$ and $n_f = 5 + |\beta|^2$. For $n_f = 6$ in Fig. 1(a), one gets a single lower ($f_{5/2}^6 \rightarrow f_{5/2}^5$) and upper ($f_{5/2}^6 \rightarrow f_{5/2}^6 f_{7/2}^1$) Hubbard band. For $n_f = 5$ in Fig. 1(c), however, one may still add an electron to the $j = 5/2$ subshell, so that in addition to

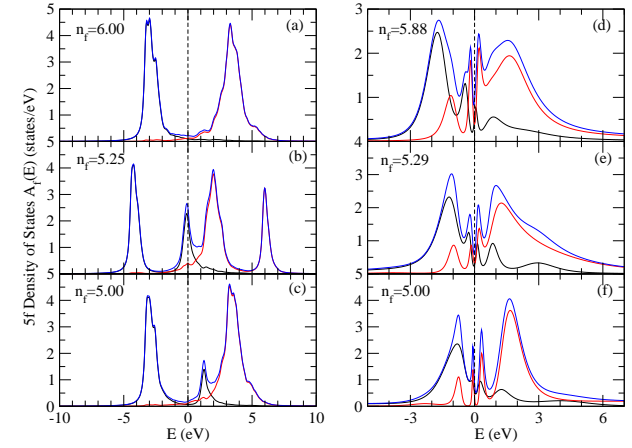


FIG. 1: (Color) The 5f spectral density calculated from the DMFT(HI) [left panels] and DMFT(QMC) [right panels] for δ -Pu for varying 5f site energy at $T = 632$ K. In all panels, the spectral density contributed from the $j = 5/2$ and $j = 7/2$ sub-shells are represented by the black and red lines, respectively. The total 5f spectral density is represented by the blue line. The energy $E = 0$ denotes the position of the Fermi level.

the lower ($f_{5/2}^5 \rightarrow f_{5/2}^4$) one has two, spin-orbit split upper Hubbard bands ($f_{5/2}^5 \rightarrow f_{5/2}^6$ and $f_{5/2}^5 \rightarrow f_{5/2}^5 f_{7/2}^1$). For the mixed valent, nonintegral n_f in Fig. 1(b), the system behaves as an ensemble of $|\alpha|^2 f_{5/2}^5$ and $|\beta|^2 f_{5/2}^6$ configurations. In the absence of hybridization, this leads to four Hubbard bands in relative position $4U_f$, $5U_f$, $5U_f + \Delta_f$, and $6U_f + \Delta_f$, where Δ_f is the spin-orbit splitting, with areas of $5|\alpha|^2$, $6|\beta|^2 + |\alpha|^2$, $8|\alpha|^2$, and $8|\beta|^2$, respectively. The Fermi level (energy zero) should lie within the second Hubbard band at $5U_f$ splitting the occupied ($6|\beta|^2$) and empty ($|\alpha|^2$) parts, where the latter is the small tail of the $j = 5/2$ spectra (black) extending above the Fermi level in Fig. 1(b).

For the more rigorous DMFT(QMC) results one sees, in the three right-hand panels of Fig. 1, the expected transfer of spectral weight away from the Hubbard bands into the quasiparticle peak at the Fermi level, which DMFT(HI) is incapable of describing. However, in addition there also appears to be a shift of the outlying DMFT(HI) Hubbard structure closer towards the Fermi level, while at the same time the one Hubbard band already overlapping the Fermi level [second from left in Fig. 1(b)] spreads away from the Fermi level. The overall effect is to give a more smooth and systematic evolution of the DMFT(QMC) spectra with growing n_f than seen in DMFT(HI). This is confirmed by an independent evaluation of the DMFT(QMC) state density at the Fermi level via $A_j(0) = (2j+1)(\beta/\pi)G_j(\tau = \beta/2)$.⁴⁴ $A_{5/2}(0)$ smoothly decreases while $A_{7/2}(0)$ (and the total) smoothly increase for increasing n_f over the range $5 \leq n_f \leq 6$, consistent with the Fermi level passing more into the $j = 7/2$ part of a spin-orbit split peak. Indeed, the MaxEnt results in Figs. 1(d-f) exhibit a splitting in

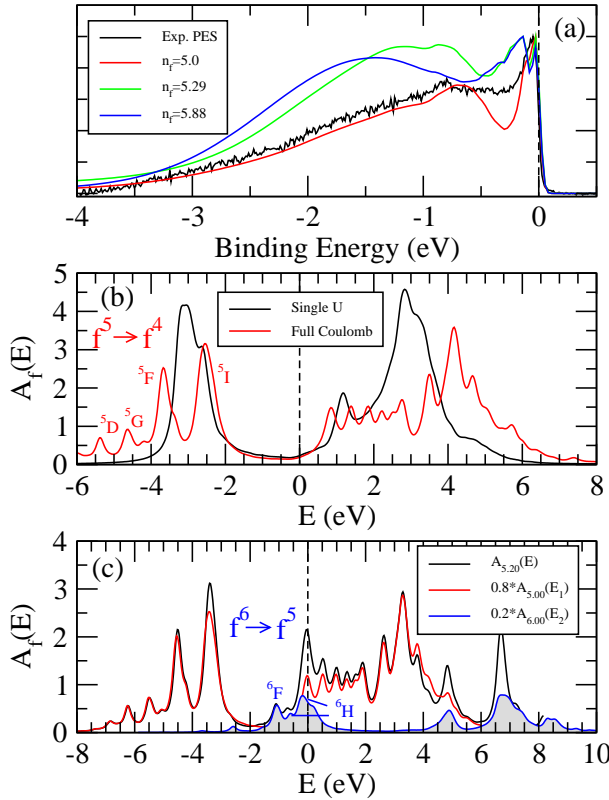


FIG. 2: (Color) (a) Experimental and theoretical photoemission spectrum. (b) The 5f spectral density calculated from the DMFT(HI) with only $F^0 = U_f$ (black line) and full Coulomb (red line) interactions for $n_f = 5.0$. (c) The 5f spectral density calculated from the DMFT(HI) with full Coulomb interactions for $n_f = 5.2$ and scaled/shifted ones for $n_f = 5.0$ and 6.0. Here $E_1 = E + 0.87$ eV and $E_2 = E - 2.29$ eV.

the quasiparticle peak. On the one hand, we suggest that it is due to the spin-orbit interaction and the associated j -dependence induced into the self-energy. Such splitting appears in the spectra for each j as the two channels couple via $\hat{H}^0(\mathbf{k})$. A reanalysis using MaxEnt of earlier DMFT(QMC) calculations⁴² for Ce and Pr exhibits similar behavior, and since this is then independent of filling, hybridization dips or gaps can be ruled out. Such spin-orbit induced splitting has been experimentally observed in photoemission experiments for Ce,⁴⁵ although the Hund's rules exchange omitted in Fig. 1 (and discussed shortly) will have larger impact for multi- f electron atoms. On the other hand, we do not exclude the possibility that the splitting may be simply an artifact of the analytical continuation technique used to obtain the spectral function at the real energy axis. Note that we find the quasiparticle peak and its associated fine structure to both disappear for δ -Pu at higher temperature, 1580 K, consistent with the 800 K Kondo energy that has been suggested.²⁸

A comparison of the DMFT(QMC) spectra with experimental photoemission data^{20,46} is shown in Fig. 2(a). The spd valence contribution was added to the calculated

5f spectra from Figs. 1(d-f), and the total was broadened to reflect the 60 meV instrument resolution and 15 K measurement temperature, as well as the Lorentzian for the photohole lifetime determining the natural linewidth, including quadratic scaling with binding energy. For the experimental comparison, data from the 40.8 eV HeII-alpha line were selected to obtain a photon energy range where orbitals of interest have similar cross sections.²⁰ While additional work is certainly needed for an optimal comparison with the data, Fig. 2(a) does reproduce the trend seen in the DMFT(QMC) results of Figs. 1(d-f), where the lower Hubbard band is seen to move to more negative energies with increasing n_f , which lends experimental support for a value of n_f closer to 5.

The implications of the comparison in Fig. 2(a) do not appear to be compromised by omitting Hund's rules exchange and the associated term structure in the theoretical results, where only the monopole Slater integral $F^0 = U_f$ has been incorporated. This can be tested in DMFT(HI), where the black curve in Fig. 2(b) is the total $n_f = 5.0$ 5f spectra of Fig. 1(c), while the red curve now treats the full Coulomb interaction taking in addition reasonable experimental values for F^2 , F^4 , and F^6 . In the electron removal spectra one now sees the standard terms (labelled) of the f^4 final state. These agree in relative position and intensity with earlier theoretical analysis,⁴⁷ and serve only to broaden the lower Hubbard band to the negative-energy side, leaving the positive-energy side of importance to the comparison in Fig. 2(a) relatively unaffected. While this DMFT(HI) test can not probe the impact of Hund's rules exchange on the quasi-particle peak near the Fermi level, one might anticipate a reduced effect after such fine structure has been appropriately broadened for comparison to photoemission data.

There has been much discussion of a three-peak structure within about 1 eV of the Fermi level in the photoemission of Pu systems: in thin layers of PuSe,⁴⁸ thin Pu layers on Mg,^{49,50} single crystal PuTe,⁵¹ and suggested in thin film of PuSi_{1.7}⁵² and PuN.⁵³ The presence of the structure in thin Pu layers (a few ML) was interpreted as a result of localization effects due to low dimensionality overcoming the itinerant character of 5f electrons.⁴⁹ More recently it has been suggested that such structure may be evident in δ -Pu metal itself.^{28,52} Such structure may also be seen in DMFT(HI) calculations including the full Coulomb interaction. In Fig. 2(c), the black curve corresponds to a DMFT(HI) calculation with the 5f site energy adjusted so $n_f = 5.2$. For comparison the red (blue/shaded) curve shows the $n_f = 5.0$ (6.0) result scaled by $|\alpha|^2 = 0.8$ ($|\beta|^2 = 0.2$) and shifted so its lowest unoccupied (highest occupied) state is at the Fermi level. The three peaks discussed are shown labelled: $^6H_{5/2}$ essentially at the Fermi level, and then $^6H_{7/2}$ and $^6F_{5/2}$ moving below. Given the agreement between the DMFT(HI) spectra $A_{5.2}$ for $n_f = 5.2$ with the composite $0.8A_{5.0} + 0.2A_{6.0}$ (addition not shown), it is evident that especially the left two peaks arise from f^5

term structure in the final state of $5f^6 \rightarrow 5f^5$ electron removal, and that the strength of these peaks might provide a direct measure of the $5f^6$ admixture β into the δ -Pu ground state, and therefore of n_f itself.

There is little doubt that such an analysis is reasonable for some Pu compounds, where precise atomic multiplet calculations were found in agreement with photoemission data in both line positions and intensities.⁴⁸ Such agreement includes cases (cubic PuTe and PuSe) where the three-peak structure is experimentally observed below the Fermi level approximately 100 meV. The situation provided by a metallic environment as in δ -Pu is substantially different, however, and so the localized multiplet interpretation is not at all clear. An obvious concern about the results in Fig. 2(c), for example, is that the self-energy used in DMFT(HI) is too atomic-like; the differences between the DMFT(HI) and DMFT(QMC) curves in Fig. 1 add to this concern.

The nature of the peak right at the Fermi level in δ -Pu is clearer. The low-temperature electronic specific heat in bulk δ -Pu metal is $64 \pm 3 \text{ mJ K}^{-2} \text{ mol}^{-1}$.⁵⁴ This large, heavy-fermion-like value indicates significant $5f$ state density at the Fermi level which is consistent with the kind of Kondo-like physics that DMFT(QMC) can yield, albeit possibly at temperatures below the present work. Corroborating evidence comes from the photon energy dependent and temperature dependent photoemission experiments performed on clean δ -Pu metal surfaces,^{20,55,56} which strongly suggest that the first peak in the δ -Pu arises from $5f$ electrons that are hybridized with the conduction electrons, which is again a typical quasiparticle feature usually found for materials with an enhanced electron mass.

IV. SUMMARY

We report a systematic LDA-DMFT study of the spectral properties of δ -Pu with varying $5f$ occupancy. The

strong sensitivity of the spectral properties to the $5f$ occupancy and the inherent ambiguity in defining the associated $5f$ orbitals suggests the need to use $5f$ occupancy as a fitting parameter in addition to the Hubbard U for DMFT theories of Pu and other materials. By comparing with photoemission data, we conclude that an “open shell” $5f^5$ configuration gives better agreement with experiment than the hypothesized “closed shell” $5f^6$ case.^{18,19,26,27} The DMFT(HI) approach, which is accurate in the localized, atomic limit, gives significantly different results from the more rigorous DMFT(QMC) method, which confirms the presence of a significant itinerant character in δ -Pu, especially at the Fermi energy. The “3-peak” structure seen within about 1 eV of the Fermi level in the photoemission spectra of some Pu compounds as well as metallic thin films, but which remains controversial for the bulk δ -Pu metal, may provide a measure of the admixture of $5f^6$ character in the ground state of these materials, and therefore an additional indication of n_f . However, it is not clear from the present work whether this structure should wash out in a correlated calculation for δ -Pu, which rigorously treats both extended and intraatomic exchange effects.

Acknowledgments

We are grateful to G. Kotliar, V. Oudovenko, S. Y. Savrasov, K. Held, and C. D. Batista for helpful discussions, and to J. E. Gubernatis and M. Jarrell for making available their maximum entropy code. We acknowledge the support of the US DOE at LANL under Contract No. DE-AC52-06NA25396, and at LLNL under Contract No. W-7405-Eng-48.

¹ O. J. Wick, *Plutonium Handbook A Guide to the Technology* (Gordon and Breach, New York, 1967).

² D. A. Young, *Phase Diagrams of the Elements* (University of California Press, Berkeley, 1991).

³ *Challenges in Plutonium Science*, edited by N. G. Cooper, special issue of Los Alamos Sci. **26** (2000).

⁴ R. C. Albers, Nature **410**, 759 (2001).

⁵ S. S. Hecker, D. R. Harbur, T. G. Zocco, Porg. Mater. Sci. **49**, 429 (2004); S. S. Hecker, MRS Bull. **26**, 672 (2001); Metall. Mater. Trans. A **35**, 2207 (2004).

⁶ R. C. Albers and Jian-Xin Zhu, Nature **446**, 504 (2007).

⁷ P. Söderlind, O. Eriksson, B. Johansson, and J. M. Wills, Phys. Rev. B **50**, 7291 (1994).

⁸ M. D. Jones, J. C. Boettger, R. C. Albers, and D. J. Singh, Phys. Rev. B **61**, 4644 (2000).

⁹ I. V. Solovyev, A. I. Liechtenstein, V. A. Gubanov, V. P. Antropov, and O. K. Andersen, Phys. Rev. B **43**, 14414 (1991).

¹⁰ Y. Wang and Y. Sun, J. Phys.: Condens. Matter **12**, L311 (2000).

¹¹ P. Söderlind, Europhys. Lett. **55**, 525 (2001).

¹² P. Söderlind, A. Landa, and B. Sadigh, Phys. Rev. B **66**, 20519 (2002).

¹³ P. Söderlind and B. Sadigh, Phys. Rev. Lett. **92**, 185702 (2004).

¹⁴ J. C. Lashley, A. Lawson, R. J. McQueeney, and G. H. Lander, Phys. Rev. B **72**, 054416 (2005).

¹⁵ J. Bouchet, B. Siberchicot, F. Jollet, and A. Pasture, J. Phys.: Condens. Matter **12**, 1723 (2000).

¹⁶ D. L. Price, B. R. Cooper, S.-P. Lim, and I. Avgin, Phys. Rev. B **61**, 9867 (2000).

¹⁷ S. Y. Savrasov and G. Kotliar, Phys. Rev. Lett. **84**, 3670 (2000).

¹⁸ A. B. Shick, V. Drchal, and L. Havela, Europhys. Lett. **69**,

588 (2005); A. B. Shick, L. Havela, J. Kolorenc, V. Drchal, T. Gouder, and P. M. Oppeneer, Phys. Rev. B **73**, 104415 (2006).

¹⁹ A. O. Shorikov, A. V. Lukoyanov, M. A. Korotin, and V. I. Anisimov, Phys. Rev. B **72**, 024458 (2005).

²⁰ J. M. Wills, O. Eriksson, A. Delin, P. H. Andersson, J. J. Joyce, T. Durakiewicz, M. T. Butterfield, A. J. Arko, D. P. Moore, and L. A. Morales, J. Electron Spectr. and Rel. Phenom. **135**, 163 (2004); O. Eriksson, D. Becker, A. V. Balatsky, and J. M. Wills, J. J. Alloys and Comp. **287**, 1 (1999).

²¹ V. I. Anisimov, A. I. Poteryaev, M. A. Korotin, A. O. Anokhin, and G. Kotliar, J. Phys.: Condens. Matter **9**, 7359 (1997).

²² For a review, see G. Kotliar, S. Y. Savrasov, K. Haule, V. S. Oudovenko, O. Parcollet, C. A. Marianetti, Rev. Mod. Phys. **78**, 865 (2006).

²³ Th. Pruschke, M. Jarrell, and J. K. Freericks, Adv. Phys. **44**, 187 (1995).

²⁴ A. Georges, G. Kotliar, W. Krauth, and M. J. Rozenberg, Rev. Mod. Phys. **68**, 13 (1996).

²⁵ S. Y. Savrasov, G. Kotliar, and E. Abrahams, Nature **410**, 793 (2001).

²⁶ L. V. Pourovskii, M. I. Katsnelson, and A. I. Lichtenstein, Phys. Rev. B **72**, 115106 (2005).

²⁷ A. Shick, J. Kolorenc, L. Havela, V. Drchal, and T. Gouder, Europhys. Lett. **77**, 17003 (2007).

²⁸ J. H. Shim, K. Haule, and G. Kotliar, Nature **446**, 513 (2007).

²⁹ K. T. Moore, G. van der Laan, R. G. Haire, M. A. Wall, and A. J. Schwartz, Phys. Rev. B **73**, 033109 (2006).

³⁰ G. van der Laan, K. T. Moore, J. G. Tobin, B. W. Chung, M. A. Wall, and A. J. Schwartz, Phys. Rev. Lett **93**, 097401 (2004)

³¹ L. V. Pourovskii, G. Kotliar, M. I. Katsnelson, and A. I. Lichtenstein, Phys. Rev. B **75**, 235107 (2007).

³² M. D. Jones and R. C. Albers, Phys. Rev. B **66**, 134105 (2002).

³³ J. C. Slater and G. F. Koster, Phys. Rev. **94**, 1498 (1954).

³⁴ W. A. Harrison, *Electronic Structure and the Properties of Solids* (Freeman, San Francisco, 1980).

³⁵ A. K. McMahan, Phys. Rev. B **58**, 4293 (1998).

³⁶ M. D. Jones and R. C. Albers, unpublished.

³⁷ A. K. McMahan, R. M. Martin, S. Satpathy, Phys. Rev. B **38**, 6650 (1988). See Eqs. (1) and (2), and Table III.

³⁸ V. I. Anisimov and O. Gunnarsson, Phys. Rev. B **43**, 7570 (1991).

³⁹ In DMFT(QMC) calculations using our constrained occupation values of both ε_f and U_f along with an LMTO-ASA $\hat{H}^{\text{LDA}}(\mathbf{k})$, we also find $n_f \sim 5$, in agreement with the spectroscopic-based conclusions of the present paper.

⁴⁰ K. Held, A. K. McMahan, and R. T. Scalettar, Phys. Rev. Lett. **87**, 276404 (2001).

⁴¹ A. K. McMahan, K. Held, and R. T. Scalettar, Phys. Rev. B **67**, 075108 (2003).

⁴² A. K. McMahan, Phys. Rev. B **72**, 115125 (2005).

⁴³ M. Jarrell and J. E. Gubernatis, Phys. Rep. **269**, 133 (1996).

⁴⁴ N. Trivedi and M. Randeria, Phys. Rev. Lett. **75**, 312 (1999).

⁴⁵ F. Patthey, B. Delley, W-D. Schneider, and Y. Baer, Phys. Rev. Lett. **55**, 1518 (1985)

⁴⁶ A. J. Arko, J. J. Joyce, L. Morales, J. Wills, J. Lashley, F. Wastin, and J. Rebizant, Phys. Rev. B **62**, 1773 (2000).

⁴⁷ F. Gerken and S. Schmidt-May, J. Phys. F: Met. Phys. **13**, 1571 (1983).

⁴⁸ T. Gouder, F. Wastin, J. Rebizant, and L. Havela Phys. Rev. Lett. **84**, 3378 (2000).

⁴⁹ T. Gouder, L. Havela, F. Wastin, and J. Rebizant Europhys. Lett. **55**, 705 (2001).

⁵⁰ L. Havela, T. Gouder, F. Wastin, and J. Rebizant Phys. Rev. B **65**, 235118 (2002).

⁵¹ T. Durakiewicz, J. J. Joyce, G. H. Lander, C. G. Olson, M. T. Butterfield, E. Guziewicz, A. J. Arko, L. Morales, J. Rebizant, K. Mattenberger, and O. Vogt, Phys. Rev. B **70**, 205103 (2004).

⁵² T. Gouder, R. Eloirdi, J. Rebizant, P. Boulet, and F. Huber, Phys. Rev. B **71**, 165101 (2005).

⁵³ L. Havela, F. Wastin, J. Rebizant, and T. Gouder Phys. Rev. B **68**, 085101 (2003).

⁵⁴ J. C. Lashley, J. Singleton, A., Migliori, J.B. Betts, R.A. Fisher, J.L. Smith, and R.J. McQueeney, Phys. Rev. Lett. **91**, 205901 (2003).

⁵⁵ J. J. Joyce, T. Durakiewicz, C. G. Olson, E. Guziewicz, K. S. Graham, D. P. Moore, L. A. Morales, Mat. Res. Soc. Symp. Proc. **986**, 35 (2007).

⁵⁶ J. J. Joyce, A. J. Arko, L. E. Cox, and S. Czuchlewski, Surface and Interface Analysis **26**, 121 (1998).